

Accepted Manuscript

Design, synthesis, structure-activity relationships and mechanism of action of new quinoline derivatives as potential antitumor agents

Shangze Li, Lihua Hu, Jianru Li, Jiongchang Zhu, Feng Zeng, Qiuhua Huang, Liqin Qiu, Runlei Du, Rihui Cao



PII: S0223-5234(18)31007-9

DOI: <https://doi.org/10.1016/j.ejmech.2018.11.048>

Reference: EJMECH 10906

To appear in: *European Journal of Medicinal Chemistry*

Received Date: 29 August 2018

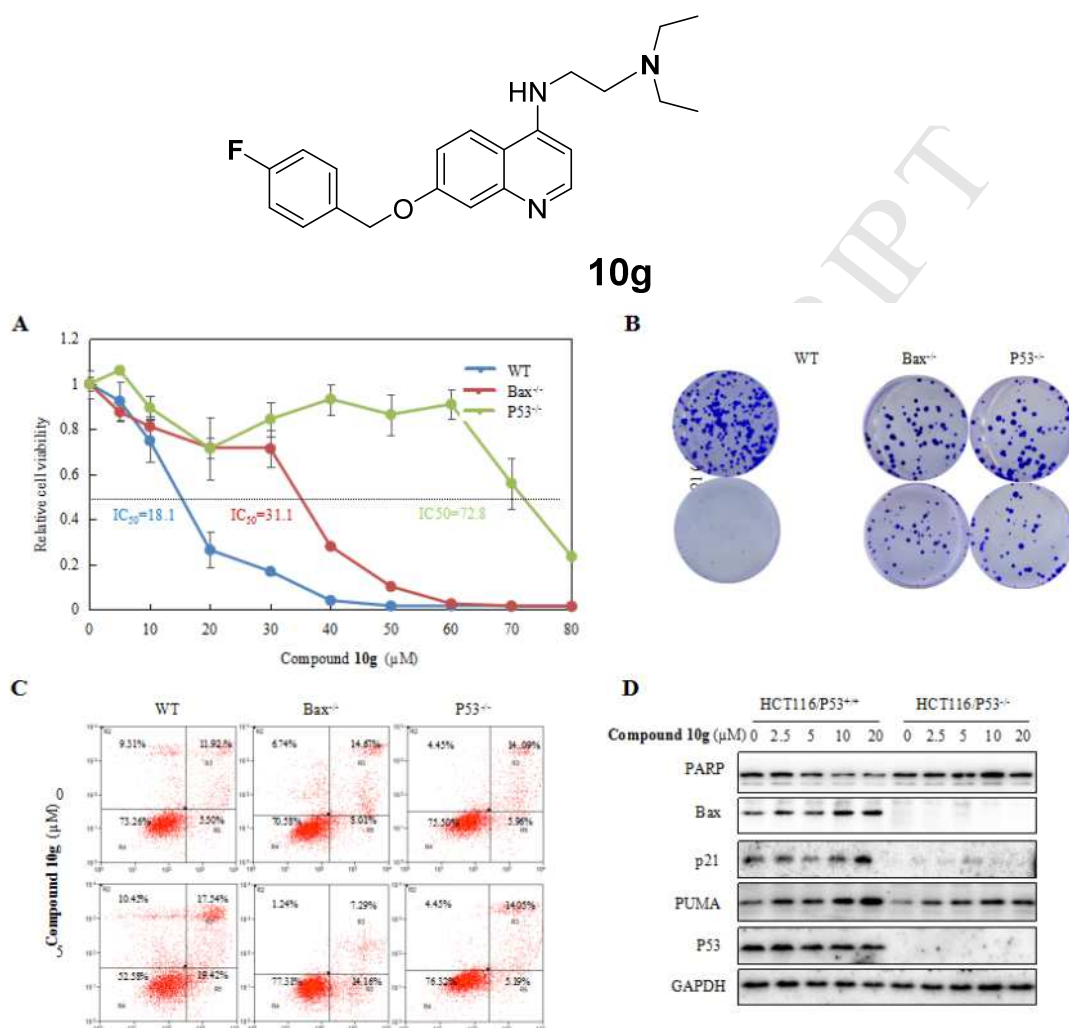
Revised Date: 18 November 2018

Accepted Date: 20 November 2018

Please cite this article as: S. Li, L. Hu, J. Li, J. Zhu, F. Zeng, Q. Huang, L. Qiu, R. Du, R. Cao, Design, synthesis, structure-activity relationships and mechanism of action of new quinoline derivatives as potential antitumor agents, *European Journal of Medicinal Chemistry* (2018), doi: <https://doi.org/10.1016/j.ejmech.2018.11.048>.

This is a PDF file of an unedited manuscript that has been accepted for publication. As a service to our customers we are providing this early version of the manuscript. The manuscript will undergo copyediting, typesetting, and review of the resulting proof before it is published in its final form. Please note that during the production process errors may be discovered which could affect the content, and all legal disclaimers that apply to the journal pertain.

Graphic abstract



A series of new quinoline derivatives was designed, synthesized and evaluated as promising antitumor agents. The representative compound **10g** could trigger p53/Bax-dependent colorectal cancer cell apoptosis by activating p53 transcriptional activity.

**Design, synthesis, structure-activity relationships and mechanism of
action of new quinoline derivatives as potential antitumor agents**

Shangze Li^{c, #}, Lihua Hu^{b, #}, Jianru Li^a, Jiongchang Zhu^a, Feng Zeng^b, Qiuhua Huang^a,

Liqin Qiu^a, Runlei Du^b, Rihui Cao^{a*}

^a*School of Chemistry, Sun Yat-sen University, 135 Xin Gang West Road, Guangzhou 510275,
P R China*

^b*College of Life Sciences, Wuhan University, 299 Ba Yi Road, Wuchang, 430072, P R China*

^c*Medical Science Research Center, Zhongnan hospital of Wuhan University, Hubei, Wuhan
430071, P R China*

*Corresponding author. Tel: 86-20-84110918 Fax: 86-20-84112245, E-mail:
caorihui@mail.sysu.edu.cn (R. Cao). # Shangze Li and Lihua Hu contributed equally to this work.

Abstract

A series of new quinoline derivatives was designed, synthesized and evaluated as potential antitumor agents. The results indicated that most compounds exhibited potent antiproliferative activity, and 7-(4-fluorobenzyloxy)-*N*-(2-(dimethylamino)ethyl)quinolin-4-amine **10g** was found to be the most potent antiproliferative agent against human tumor cell lines with an IC₅₀ value of less than 1.0 μM. Preliminary structure-activity relationships analysis suggested that (1) the large and bulky alkoxy substituent in position-7 might be a beneficial pharmacophoric group for antiproliferative activity; (2) the amino side chain substituents in position-4 facilitated the antiproliferative activity of this class of compounds; and (3) the length of the alkylamino side chain moiety affected the antiproliferative potency, with two CH₂ units being the most favorable. Further investigation of the mechanism of action of this class of compounds demonstrated that the representative compound **10g** triggered p53/Bax-dependent colorectal cancer cell apoptosis by activating p53 transcriptional activity. Moreover, the results showed that compound **10g** effectively inhibited tumor growth in a colorectal cancer xenograft model in nude mice. Thus, these quinoline derivatives might serve as candidates for the development of new antitumor drugs.

Key Words: Synthesis; quinoline derivative; antiproliferative; structure-activity relationships; mechanism of action.

1. Introduction

Apoptosis is a programmed cellular suicide process that can remove damaged cells, such as cancer cells, from multicellular organisms. In cancer cells, the apoptotic pathway is often inactivated at the cellular level, which results in drug resistance in cancer[1]. Therefore, developing a strategy to increase apoptosis activity is a potential approach for cancer therapy.

The transcription factor p53 mediates multiple biological processes, such as cell cycle arrest, apoptosis, metabolism and autophagy[2]. Over half of patients with tumors have mutation of p53 protein, and thus, p53 is considered to be crucial for suppressing tumorigenesis[3]. The post-translational modifications, including phosphorylation, acetylation, ubiquitination and sumoylation, are the primary mechanism by which p53 is regulated. Phosphorylation of p53 at several serine/threonine residues has been shown to promote nuclear localization, stabilization, DNA binding and subsequent transcriptional activation. Induction of apoptotic death in cancer cells is considered the major mechanism by which p53 prevents tumor development and progression.

Quinolines represent a large group of naturally occurring and synthetic products associated with a wide spectrum of pharmacological functions, including antibacterial[4-6], antitumor[7-9] and anti-HIV[10] activities. Since the discovery of nalidixic acid by Lesher in 1962, intense research efforts have been spent in search of more potent antibacterial agents, and the structure-activity relationships of quinolines as antibacterial agents have also been extensively investigated[5-7, 9, 11].

Initially, quinolines were found to be specific inhibitors of bacterial type II

topoisomerases, such as DNA gyrase[12]. Recently, topoisomerase IV[13], Pim-1 kinase[14], EGFR tyrosine kinase[15], tyrosine-protein kinase Met (c-Met)[16], Penicillin-Binding Proteins[17] and histone deacetylase (HDAC)[18] were also discovered to be pharmacological targets of this class of compounds. Due to structural and functional similarities between bacterial DNA gyrase and human topoisomerase II, it is speculated that this class of compounds also have potential antitumor activity. Consequently, in the past decade, considerable attention has been focused on the antitumor effects of quinolines, and a larger number of quinolines have been reported as promising antitumor agents[7, 14-16, 19-26].

Antitume, 7-chloro-4(1H)-quinolone **11** (**Fig. 1**), was approved by the State Food and Drug Administration of China (SFDA) as an antitumor drug for late mammary cancer and non-small cell lung cancer treatment in 2003[27]. The advantage of this compound as an antitumor drug is its low toxicity, easy administration and cheap synthesis. However, its poor solubility and moderate antitumor activity *in vivo* have limited its wide application in clinical cancer therapy. Our group recently demonstrated that introducing a flexible amino side chain into position-3 of the quinoline nucleus contributes to improving the water solubility and *in vitro* antiproliferative activity of this class of compounds[28]. In a continuing effort to develop novel quinoline derivatives endowed with better pharmacological profiles, we designed and synthesized a series of new quinolines bearing an alkoxy group in position-7 as well as a flexible alkylamino side chain at position-4. Herein, we report the preparation of new quinoline derivatives, their antiproliferative activity,

preliminary structure-activity relationships and mechanism of action as antitumor agents.

2. Chemistry

The synthetic routes of quinolines **7**, **9a-k** and **10a-h** are outlined in **Scheme 1**. The reaction of *m*-anisidine **1** with ethoxymethylenemalononic ester **2** afforded the crude Schiff base **3**[29]. Cyclization of intermediate **3** in refluxing diphenyl ether gave carboxylate **4**[29], followed by hydrolysis with 10% sodium hydroxide solution to provide carboxylic acid **5**[29]. Decarboxylation of carboxylic acid **5** in refluxing diphenyl ether afforded 7-methoxyquinolin-4(1H)-one **6**. The conversion of **6** to 4-chloro-7-methoxy-quinoline **7** occurred readily by treatment with phosphorous oxychloride. The demethylation of 4-chloro-7-methoxy-quinoline **7** was accomplished readily using 48% hydrobromic acid as the reaction solvent to give 4-chloroquinolin-7-ol **8**[30]. Compounds **9a-k** bearing various alkoxy groups in position-7 of the quinoline nucleus were synthesized from intermediate **8** by the action of sodium hydride in dry DMF followed by addition of the appropriate alkylating and arylating agents[30]. The amination of **9a**, **9c**, **9f**, **9h** and **9i** with an excess of *N,N*-diethylethylenediamine or 3-(diethylamino)propylamine by refluxing provided the target compounds **10a-h** in good yields[31]. The chemical structure of all the synthesized new compounds was characterized by ESI-MS, HRMS, ¹H NMR and ¹³C NMR.

3. Results and Discussion

3.1 Antiproliferative activity *in vitro*

The antiproliferative activity of quinolone derivatives **7**, **9a-k** and **10a-h** against a panel of human tumor cell lines was investigated and compared with the reference drug cisplatin. To improve the solubility in aqueous solution, all compounds were prepared in the form of hydrochloride by the usual methods before use. The compounds **10a-h** showed good water solubility (more than 10mg/mL). The tumor cell line panel consisted of human colorectal carcinoma (HCT-116, RKO and DLD1), liver carcinoma (HepG2), gastric carcinoma (BGC-823), non-small-cell lung carcinoma (NCI-H1650) and ovarian carcinoma (SK-OV-3) cells. The results are summarized in **Table 1**.

As shown in **Table 1**, the lead compound 7-chloro-4(1H)-quinolone **11** failed to display antiproliferative activity against human tumor cell lines at a concentration of 10 μ M. Compound **7** bearing a methoxy group in position-7 of the quinoline nucleus only showed selective antiproliferative activity against the HCT-116, RKO, HepG2 and NCI-H1650 human tumor cell lines, with IC_{50} values of 8.82, 9.65, 6.07 and 8.16 μ M, respectively. However, compounds **9a-k** having relatively large and bulky alkoxy substituents in position-7 displayed more potent antiproliferative activity against several human tumor cell lines, with IC_{50} values of lower than 5.0 μ M. Among all the 7-alkoxy substituted quinoline derivatives **9a-k**, compound **9k** exhibited the most interesting antiproliferative activity against the HCT-116 and NCI-H1650 human tumor cell lines, with IC_{50} values of 0.80 and 0.63 μ M, respectively. These results suggested that a large and bulky substituent at position-9 might be advisable pharmacophoric group for antiproliferative activities.

Our group previous investigations[28, 31-34] demonstrated that introducing a flexible amino side chain into various skeleton molecules contributes to improving the water solubility and *in vitro* antiproliferative activity. Logically, we speculated that introducing an aminoethylamino side chain group into position-4 of quinolines **9** would impart improved water solubility and enhanced antiproliferative activity. Consequently, a series of novel quinolone derivatives **10a-h** bearing a flexible amino side chain with a two or three methylene spacer in position-4 were prepared. As predicted, most of the compounds exhibited more potent antiproliferative potency against human tumor cell lines, with IC_{50} values lower than 2.0 μM . Although the antiproliferative potency of compounds **10-b** bearing an ethoxy group in position-7 showed no distinct difference with their parent compound **9a**, compounds **10c**, **10e** and **10g** displayed more potent antiproliferative activity than their parent compounds **9b**, **9f** and **9i**, with IC_{50} values ranging from 0.37 to 1.86 μM . Interestingly, compounds **10c**, **10e** and **10g** bearing a flexible amino side chain with a two methylene spacer displayed more potent cytotoxic potency than compounds **10d**, **10f** and **10h**, which contained a three methylene spacer. Particularly, compound **10g**, bearing a 4-fluorobenzyl group in position-7 and a flexible amino side chain with a two methylene spacer in position-4, was found to be the most potent antiproliferative agent, with IC_{50} values lower than 1.0 μM against all the human tumor cell lines. These results indicated that (1) the amino side chain substituents were beneficial pharmacophoric groups for enhancing the antiproliferative activity and (2) the length of the alkylamino side chain moiety affected their antiproliferative potency, with two

CH₂ units being more favorable.

3.2 Growth inhibition of human colorectal cancer cells by compound 10g

To investigate the inhibition effects of compound **10g** on cell viability and cell proliferation, we performed CCK8 and colony formation assays. The results of CCK8 assays showed that compound **10g** decreased the viability of HCT116, RKO and DLD1 cells in a time-dependent manner (**Fig. 2A**). The number of colony units decreased significantly with an increase in compound **10g** concentration (**Fig. 2B**). In addition, phase-contrast micrographs revealed that compound **10g** induced cell morphology alterations, such as cell shrinkage and reduced cell number (**Fig. 2C**).

To assess whether compound **10g** could kill cancer cells more effectively than normal cells, we examined the susceptibility of normal human colorectal and hepatic cell lines to compound **10g**. Unexpectedly, compound **10g** did not induce an obvious difference in viability between cancer cells and normal cells (FHC) in colorectal cancer cells, except at a high dose of compound **10g** (**Fig. 2D**). These experiments confirmed that compound **10g** had significant inhibitory effects on human colorectal cancer cells *in vitro*.

3.3 Compound 10g induced apoptosis in HCT116 cells

Drugs often elevate the activity of apoptosis pathways to exert anticancer effects. We first examined whether compound **10g** could induce apoptosis in HCT116 colorectal cancer cells. PI and Annexin V double staining was carried out to quantitatively evaluate apoptosis, and obviously increased early and late phase apoptosis were induced by compound **10g** in a dose-dependent manner (**Fig. 3A**).

Next, we analyzed markers of apoptosis at the protein level. Immunoblot analysis showed increased cleaved Proline-rich acidic protein (PARP) and decreased pro-caspase3 and pro-caspase9 after exposure to different doses of compound **10g** (**Fig. 3B**). Caspases play an important role in apoptosis progression as effectors. To further verify whether compound **10g**-induced apoptotic cell death was caspase dependent, z-VAD-fmk, a general caspase inhibitor, was used. As shown in **Fig. 3C**, the apoptosis induced by compound **10g** was reversed by treatment with the pan-caspase inhibitor z-VAD-fmk. The level of the apoptosis marker cleaved PRAP was also reduced after addition of z-VAD-fmk (**Fig. 3D**). These results revealed that compound **10g** induces caspase-dependent apoptosis in colorectal cancer cells.

3.4 Compound 10g-induced cell death is independent on ROS and autophagy

In addition to apoptosis, inducing intracellular ROS accumulation, autophagy and cell cycle arrest can also reduce cancer cell growth and viability[35-37]. To test whether compound **10g**-induced cell growth inhibition is exclusively dependent on apoptosis, we performed experiments to test these three biological processes. We constructed an HCT116 colorectal cancer cell line that stably expressed GFP-LC3 to determine whether compound **10g** could induce GFP-LC3 puncta. Moderate and relatively high concentrations of compound **10g** were chosen to treat the cells for 24 h. Although we observed a few GFP-LC3 puncta when the cells were exposed to 10 μ M compound **10g**, it was not sufficient to strongly induce cell death (**Fig. 4A**).

To test if the ROS level is changed after treatment with compound **10g**, we used DCFH-DA to stain cells treated with 5 or 10 μ M compound **10g**. Flow cytometry

analysis showed that the fluorescence intensity in compound **10g** treated cells was not altered compared with untreated cells; however, the positive control cells displayed an obvious elevation in ROS levels (**Fig. 4B**). This suggests that compound **10g** has no effect on ROS production at a concentration of 5 or 10 μ M.

We use PI stain to analysis cell cycle progression, and the effect of 5 μ M compound **10g** on cell cycle distribution was analyzed at 24 and 48 h via flow cytometry. An obvious change in cell cycle arrest was not observed compared with the vehicle group under these conditions (**Fig. 4C and 4D**).

3.5 Apoptosis was induced by compound 10g by targeting of p53 transcriptional activity

p53 and Bax play crucial roles in the intrinsic apoptosis pathway[38, 39]. To further investigate the possible mechanism by which compound **10g** induces apoptosis, p53- and Bax-deficient HCT116 cells were used to determine cell viability after exposure to compound **10g**. Interestingly, p53-deficient HCT116 cells displayed tremendous resistance to compound **10g**, and as the downstream gene of p53, Bax deficiency also showed moderate resistance to compound **10g**-induced apoptosis (**Fig. 5A**). Colony formation assays showed results consistent with the cell viability assays (**Fig. 5B**). Furthermore, the increase in the number of Annexin V-positive cells induced by 5 μ M compound **10g** was significantly blocked in p53- and Bax-deficient HCT116 cells (**Fig. 5C**). Immunoblotting showed that the protein levels of the p53 target genes.

Bax, PUMA and p21 were significantly increased and that of PARP was

decreased after treatment with increasing doses of compound **10g**, but this was not observed in the p53-deficient HCT116 cells (**Fig. 5D**). These results show that compound **10g**-induced cell apoptosis is dependent on p53. We noted that the protein level of p53 was not changed after exposure to compound **10g** (**Fig. 5D**), which implies that the transcriptional activity of p53 may be regulated by this compound. Because the phosphorylation and location of p53 is indicative of the transcriptional activity, we next investigated whether the phosphorylation and location of p53 is changed after treatment with compound **10g**. Phosphorylation at serines 15 and 392 of p53 regulates p53 activation and DNA binding ability[40, 41]. Therefore, we determined whether phosphorylation of these two sites is induced by compound **10g**. As shown in **Fig. 5E**, the phosphorylation of p53 at serine 15 and 392 was increased when cells were treated with compound **10g** for the indicated times (**Fig. 5E**).

To study the subcellular localization of p53, fractionation analysis was employed, and HCT116 cells were exposed to different doses of compound **10g**. As shown in **Fig. 5F**, the protein level of p53 was increased in the nucleus after exposure to compound **10g** for different time courses. Collectively, these results suggest that compound **10g** could exclusively induce p53-dependent cell apoptosis by targeting p53 transcriptional activity.

3.6 Compound 10g displays antitumor activity in vivo

To examine whether compound **10g** induced apoptosis would result in anticancer effects *in vivo*, we used a xenograft mouse model. The tumors grew quickly in control group mice who were only treated with vehicle; however, more than half the tumor

growth was suppressed in mice treated with compound **10g** at an 80 mg/kg dose. Tumor weight was significantly reduced after compound **10g** treatment (**Fig. 6A** and **6B**). These results suggested that compound **10g** could exhibit antitumor activity *in vivo*.

4. Conclusions

A series of quinolone derivatives were designed, synthesized and evaluated as promising antiproliferative agents on the basis of the chemical structure of the lead compound 7-chloro-4(1H)-quinolone **11**. Preliminary structure-activity relationship analysis indicated that (1) a large and bulky substituent in position-7 might be a beneficial pharmacophoric group for antiproliferative activity; (2) the amino side chain substituents facilitated antiproliferative activity; and (3) the length of the alkylamino side chain moiety affected the antiproliferative potency, with two CH₂ units being more favorable.

Numerous anti-cancer drugs induce cancer cell apoptosis *via* modulation of the p53 pathway. However, p53 mutations are frequent not only in colorectal cancer but also in the majority of other human tumors[42-44]. Bax also serves as an essential effector of the mitochondrial apoptotic pathway and p53-mediated apoptosis. Induction of p53 and/or Bax-dependent apoptosis by drugs has been used as a strategy to kill cancer cells[45-47]. Our investigation demonstrated that compound **10g** could trigger p53/Bax-dependent colorectal cancer cell apoptosis by activating p53 transcriptional activity. In addition, compound **10g** was found to significantly abrogate tumorigenicity in a xenograft model.

5. Experimental Section

5.1 Reagents and general methods

Z-VAD (OMe)-FMK (HY-16658) was purchased from MedChem Express. Rabbit monoclonal antibodies against Bax (#5023) and Caspase 3 (#9665) and rabbit polyclonal antibodies against Caspase 9 (#9502), cleaved PARP (#9541), p21, PUMA, p-p53(ser15), and p-p53(ser392) were obtained from Cell Signaling Technology (Beverly, MA). The antibody against total PARP and anti-mouse p53 monoclonal antibody (sc-126) were purchased from Santa Cruz Biotechnology. Antibodies targeting GAPDH and LaminA/C and the anti-mouse monoclonal β -Tubulin antibody (AbM59005-37B-PU) were obtained from BPI.

ESI-MS spectra were obtained with a VG ZAB-HS spectrometer. ^1H NMR and ^{13}C NMR spectra were recorded on a Mercury-Plus 300 spectrometer at 300 MHz and 75 MHz, respectively, using TMS as the internal standard and CDCl_3 or DMSO-d_6 as the solvent; chemical shifts (δ) are expressed in ppm. HRMS spectra were obtained with an ESI-Q-TOF maxis 4G spectrometer. All reactions were monitored by TLC, and spots were visualized with UV light. Silica gel F254 was used for analytical thin-layer chromatography (TLC), and silica gels were used for column chromatography.

5.2. Preparation of 7-methoxy-4-oxo-1,4-dihydroquinoline-3-carboxylic acid (5)

A mixture of ethyl 7-methoxy-4-oxo-1,4-dihydroquinoline-3-carboxylate **4** (20 mmol), NaOH (80 mmol), ethanol (100 mL) and H_2O (200 mL) was refluxed for 2 h, and the ethanol was removed on a rotary evaporator. The mixture was acidified with

dilute HCl. The precipitate was collected, washed well with H₂O and dried in a vacuum to provide compound **5**. Compound **5** prepared in this manner was used directly in the next step without further purification.

5.3 7-Methoxyquinolin-4(1H)-one (**6**)

A mixture of 7-methoxy-4-oxo-1,4-dihydroquinoline-3-carboxylic acid **5** (10 mmol) and diphenyl ether (30 mL) was heated under reflux for 1 h. Then, the reaction mixture was allowed to cool to room temperature, and petroleum ether (20 mL) was added. The precipitate formed was collected by filtration and washed well with petroleum ether. The pure 4-oxoquinoline **6** was obtained by recrystallization from a large amount of hot water as white needle crystals (1.6 g, 86%). ESI-MS *m/z* 176 [M+H]⁺. ¹H NMR (300 MHz, DMSO-*d*₆): δ 11.63 (1H, s, **NH**), 7.93 (1H, d, *J*= 8.7 Hz, **ArH**), 7.76 (1H, d, *J*= 7.5 Hz, **ArH**), 6.91 (1H, d, *J*=2.4 Hz, **ArH**), 6.88 (1H, dd, *J*= 8.7 Hz, *J*= 2.4 Hz, **ArH**) 5.91 (1H, d, *J*= 7.5 Hz, **ArH**), 3.83(3H, s, **CH**₃).

5.4 4-Chloro-7-methoxyquinoline (**7**)

A mixture of 7-methoxyquinolin-4(1H)-one **6** (10 mmol) and phosphorous oxychloride (30 mL) was heated for 3 h. Most of phosphorous oxychloride was removed by evaporation under reduced pressure, and the residue was poured into ice water. Then, the mixture was made alkaline with ammonium hydroxide; the precipitate formed was collected by filtration, washed well with water and dried in a vacuum; and compound **7** was obtained as white solid (1.7 g, 88%). ESI-MS *m/z* 194 [M+H]⁺. ¹H NMR (300 MHz, CDCl₃): δ 8.67 (1H, d, *J*= 4.8 Hz, **ArH**), 8.09 (1H, d, *J*= 9.0 Hz, **ArH**), 7.42 (1H, d, *J*=2.4 Hz, **ArH**), 7.33 (1H, d, *J*=4.8 Hz, **ArH**), 7.28 (1H,

dd, $J=9.0$ Hz, $J=2.4$ Hz, ArH), 3.97 (3H, s, CH₃). ¹³C NMR (75 MHz, CDCl₃) δ 161.3, 151.0, 150.2, 142.4, 125.3, 121.7, 120.8, 119.3, 107.7, 55.9.

5.5 Preparation of 4-chloroquinolin-7-ol (**8**)

A mixture of 4-chloro-7-methoxyquinoline **7** (1.93 g, 10 mmol) and 48% hydrobromic acid (50 mL) was refluxed. After completion of the reaction as indicated by TLC, the mixture was cooled and poured onto ice. The aqueous mixture was alkalized to pH 6 using 10% NaOH solution. The resulting precipitate was filtered, washed with water and dried in vacuum to give **8** (1.76 g, 98%). The material was used without further purification for the following step.

5.6 General procedure for compounds **9a-k**

A mixture of 4-chloroquinolin-7-ol **8** (0.72 g, 4 mmol) and anhydrous DMF (10 mL) was stirred at room temperature until clear, and then, 60% NaH (0.4 g, 10 mmol) and halogenated alkane (20-30 mmol) were added. The mixture was stirred at room temperature. After completion of the reaction as indicated by TLC, the solution was poured into H₂O (100 mL) and extracted with ethyl acetate. The organic phase was made acidic with concentrated hydrochloric acid. Upon removal of solvent, the residue was crystallized from acetone to afford a yellow solid. The solid was dissolved in water and made basic with sodium bicarbonate, and the aqueous mixture was extracted with ethyl acetate. The organic phase was washed with water and brine and then dried over anhydrous sodium sulfate, filtered and evaporated. The resulting oil was purified by column chromatography using a mixture of dichloromethane and methanol 100:1 as the eluent to successfully afford the target products **9a-k** in good

yield.

5.6.1 4-Chloro-7-ethoxyquinoline (9a)

Starting from ethyl bromide (15 mmol), compound **9a** was isolated as a yellow solid (0.56 g, 68%), mp 70-71°C. ESI-MS m/z $(M+H)^+$ 207.8. 1H NMR (300 MHz, $CDCl_3$): δ 8.66 (1H, d, $J=4.8$ Hz, ArH), 8.09 (1H, d, $J=9.0$ Hz, ArH), 7.39 (1H, d, $J=1.8$ Hz, ArH), 7.32 (1H, d, $J=4.8$ Hz, ArH), 7.29-7.20 (1H, m, ArH), 4.19 (2H, q, $J=6.9$ Hz, CH_2), 1.50 (3H, t, $J=6.9$ Hz, CH_3). ^{13}C NMR (75 MHz, $CDCl_3$): δ 160.3, 150.6, 149.8, 142.0, 124.9, 121.2, 120.7, 118.8, 107.8, 63.7, 14.6. HRMS (ESI) calcd for $C_{11}H_{11}ClNO$ $[M+H]^+$ 208.0524, found 208.0515.

5.6.2 4-Chloro-7-isopropoxyquinoline (9b)

Starting from 2-bromopropane (30 mmol), compound **9b** was isolated as a yellow solid (0.48 g, 54%), mp 65-66°C. ESI-MS m/z $[M+H]^+$ 221.8. 1H NMR (300 MHz, $CDCl_3$): δ 8.65 (1H, d, $J=4.8$ Hz, ArH), 8.08 (1H, d, $J=9.3$ Hz, ArH), 7.39 (1H, s, ArH), 7.30 (1H, d, $J=4.8$ Hz, ArH), 7.27-7.20 (m, 1H, ArH), 4.82-4.67 (1H, m, CH), 1.43 (6H, d, $J=6.0$ Hz, CH_3). ^{13}C NMR (75 MHz, $CDCl_3$): δ 159.3, 150.5, 149.7, 142.1, 125.0, 121.5, 121.0, 118.7, 108.8, 70.2, 21.7. HRMS (ESI) calcd for $C_{12}H_{13}ClNO$ $[M+H]^+$ 222.0680, found 222.0676.

5.6.3 7-(Allyloxy)-4-chloroquinoline (9c)

Starting from allyl bromide (20 mmol), compound **9c** was isolated as a yellow solid (0.69 g, 79%), mp 36-37°C. ESI-MS m/z $(M+H)^+$ 219.8. 1H NMR (300 MHz, $CDCl_3$): δ 8.66 (1H, d, $J=4.5$ Hz, ArH), 8.09 (1H, d, $J=9.0$ Hz, ArH), 7.41 (1H, s, ArH), 7.29 (2H, dd, $J=16.0$ Hz, $J=6.3$ Hz, ArH), 6.10-6.16 (1H, m, $CH_2=CH$), 5.48

(1H, d, $J = 17.2$ Hz, $\text{CH}_2=\text{CH}$), 5.34 (1H, d, $J = 10.5$ Hz, $\text{CH}_2=\text{CH}$), 4.69 (2H, d, $J = 4.8$ Hz, OCH_2). ^{13}C NMR (75 MHz, CDCl_3): δ 159.9, 150.5, 149.9, 142.1, 132.2, 125.1, 121.4, 120.8, 119.0, 118.1, 108.4, 68.9. HRMS (ESI) calcd for $\text{C}_{12}\text{H}_{10}\text{ClNO}$ $[\text{M}+\text{H}]^+$ 220.0524, found 220.0535.

5.6.4 4-Chloro-7-butoxyquinoline (9d)

Starting from 1-bromobutane (30 mmol), compound **9d** was isolated as a yellow solid (0.46 g, 49%), mp 37-38 $^\circ$. ESI-MS m/z $[\text{M}+\text{H}]^+$ 236.1. ^1H NMR (300 MHz, CDCl_3): δ 8.65 (1H, d, $J = 4.8$ Hz, ArH), 8.08 (1H, d, $J = 9.3$ Hz, ArH), 7.39 (1H, d, $J = 1.8$ Hz, ArH), 7.31 (1H, d, $J = 4.8$ Hz, ArH), 7.29-7.23 (1H, m, ArH), 4.12 (2H, t, $J = 6.6$ Hz, CH_2), 1.92-1.79 (2H, m, CH_2), 1.62-1.47 (m, 2H, CH_2), 1.00 (3H, t, $J = 7.2$ Hz, CH_3). ^{13}C NMR (75 MHz, CDCl_3): δ 160.5, 150.7, 149.8, 142.0, 124.9, 121.2, 120.8, 118.8, 108.0, 68.0, 31.0, 19.2, 13.8. HRMS (ESI) calcd for $\text{C}_{13}\text{H}_{14}\text{ClNO}$ $[\text{M}+\text{H}]^+$ 236.0837, found 236.0844.

5.6.5 4-Chloro-7-isobutoxyquinoline (9e)

Starting from 1-bromo-2-methylpropane (30 mmol), compound **9e** was isolated as a white solid (0.84 g, 89%), mp 57-58 $^\circ$. ESI-MS m/z $[\text{M}+\text{H}]^+$ 235.8. ^1H NMR (300 MHz, CDCl_3): δ 8.65 (1H, d, $J = 4.8$ Hz, ArH), 8.09 (1H, d, $J = 9.3$ Hz, ArH), 7.38 (1H, d, $J = 2.4$ Hz, ArH), 7.31 (1H, d, $J = 4.8$ Hz, ArH), 7.28 (1H, dd, $J = 9.2$ Hz, $J = 2.4$ Hz, ArH), 3.88 (2H, d, $J = 6.5$ Hz, CH_2), 2.18 (1H, dp, $J = 13.2$ Hz, $J = 6.6$ Hz, CH), 1.07 (6H, d, $J = 6.7$ Hz, CH_3). ^{13}C NMR (75 MHz, CDCl_3): δ 160.7, 150.8, 149.9, 142.2, 125.0, 121.3, 121.0, 118.9, 108.1, 74.7, 28.1, 19.3. HRMS (ESI) calcd for $\text{C}_{13}\text{H}_{14}\text{ClNO}$ $[\text{M}+\text{H}]^+$ 236.0837, found 236.0851.

5.6.6 4-Chloro-7-(hexyloxy)quinoline (9f)

Starting from 1-bromohexane (30 mmol), compound **9f** was isolated as a yellow oil (0.72 g, 68%). ESI-MS m/z (M+H)⁺ 263.9. ¹H NMR (300 MHz, CDCl₃): δ 8.65 (1H, d, J = 4.8 Hz, ArH), 8.07 (1H, d, J = 9.0 Hz, ArH), 7.38 (1H, d, J = 2.4 Hz, ArH), 7.30 (1H, d, J = 4.8 Hz, ArH), 7.26 (1H, dd, J = 9.0 Hz, J = 2.4 Hz, ArH), 4.11 (2H, t, J = 6.6 Hz, CH₂(CH₂)₄CH₃), 1.94-1.79 (2H, m, CH₂CH₂[CH₂]₃CH₃), 1.49 (2H, m, [CH₂]₂CH₂[CH₂]₂CH₃), 1.37 (4H, m, [CH₂]₃CH₂CH₂CH₃), 0.91 (3H, t, J = 6.9 Hz, CH₃). ¹³C NMR (75 MHz, CDCl₃): δ 160.7, 150.8, 149.9, 142.2, 125.0, 121.3, 121.0, 118.9, 108.1, 68.4, 31.6, 29.0, 25.8, 22.7, 14.1. HRMS (ESI) calcd for C₁₅H₁₈ClNO [M+H]⁺ 264.1150, found 264.1159.

5.6.7 4-Chloro-7-(octyloxy)quinoline (9g)

Starting from 1-bromooctane (30 mmol), compound **9g** was isolated as a yellow oil (0.87 g, 75%). ¹H NMR (400 MHz, CDCl₃) δ 8.68 (d, J = 4.8 Hz, 1H, ArH), 8.11 (d, J = 9.2 Hz, 1H, ArH), 7.41 (d, J = 1.6 Hz, 1H, ArH), 7.33 (d, J = 4.8 Hz, 1H, ArH), 7.27 (d, J = 3.6 Hz, 1H, ArH), 4.12 (t, J = 6.4 Hz, 2H, CH₂(CH₂)₆CH₃), 1.92 – 1.81 (m, 2H, CH₂CH₂(CH₂)₅CH₃), 1.55 – 1.45 (m, 2H, CH₂CH₂CH₂(CH₂)₄CH₃), 1.42 – 1.22 (m, 8H, CH₂CH₂CH₂(CH₂)₄CH₃), 0.89 (t, J = 6.4 Hz, 3H, CH₂(CH₂)₆CH₃). ¹³C NMR (100 MHz, CDCl₃) δ 160.7, 150.8, 149.9, 142.2, 125.0, 121.3, 121.0, 118.9, 107.9, 68.3, 31.8, 29.4, 29.2, 29.0, 26.0, 22.7, 14.1. HRMS (ESI) calcd for C₁₇H₂₂ClNO [M+H]⁺ 292.1463, found 292.1465.

5.6.8 7-Benzyloxy-4-chloro-quinoline (9h)

Starting from benzyl bromide (15 mmol), compound **9h** was isolated as a white solid (0.50 g, 47%), mp 87-88°. ESI-MS m/z $[M+H]^+$ 269.8. 1H NMR (300 MHz, $CDCl_3$): δ 8.67 (1H, d, $J=4.8$ Hz, ArH), 8.12 (1H, d, $J=9.3$ Hz, ArH), 7.52-7.30 (8H, m, ArH), 5.21 (2H, s, CH_2Ph). ^{13}C NMR (75 MHz, $CDCl_3$): δ 160.2, 150.7, 150.0, 142.2, 135.9, 128.5, 128.1, 127.5, 125.2, 121.6, 120.9, 119.2, 108.7, 70.3. HRMS (ESI) calcd for $C_{16}H_{13}ClNO$ $[M+H]^+$ 270.0680, found 270.0678.

5.6.9 7-(4-Fluorobenzoyloxy)-4-chloro-quinoline (9i)

Starting from 4-fluorobenzyl bromide (20 mmol), compound **9i** was isolated as a yellow solid (1.02 g, 89%), mp 98-99°. ESI-MS m/z $[M+H]^+$ 287.9. 1H NMR (300 MHz, $CDCl_3$): δ 8.67 (1H, d, $J=4.8$ Hz, ArH), 8.12 (1H, d, $J=9.3$ Hz, ArH), 7.49-7.42 (3H, m, ArH), 7.36-7.30 (2H, m, ArH), 7.08 (2H, t, $J=8.7$ Hz, ArH), 5.17 (2H, s, CH_2Ph). ^{13}C NMR (75 MHz, $CDCl_3$): δ 162.4 (d, $J=246.4$ Hz), 159.9, 150.6, 150.0, 142.2, 131.7 (d, $J=2.2$ Hz), 129.4 (d, $J=8.1$ Hz), 125.2, 121.6, 120.8, 119.2, 115.44 (d, $J=21.5$ Hz), 108.6, 69.5. HRMS (ESI) calcd for $C_{16}H_{12}ClFNO$ $[M+H]^+$ 288.0586, found 288.0587.

5.6.10 4-Chloro-7-(phenethyloxy)quinoline (9j)

Starting from (2-bromoethyl)benzene (20 mmol), compound **9j** was isolated as a yellow solid (0.26 g, 23%), mp 84-85°. ESI-MS m/z $[M+H]^+$ 283.8. 1H NMR (300 MHz, $CDCl_3$): δ 8.64 (1H, d, $J=3.9$ Hz, ArH), 8.07 (1H, d, $J=9.0$ Hz, ArH), 7.40 (1H, s, ArH), 7.36-7.19 (7H, m, ArH), 4.34 (2H, t, $J=6.7$ Hz, OCH_2CH_2), 3.18 (2H, t, $J=6.6$ Hz, OCH_2CH_2). ^{13}C NMR (75 MHz, $CDCl_3$): δ 160.1 150.6, 149.8, 142.0, 137.7, 128.7, 128.3, 126.4, 124.9, 121.3, 120.7, 118.9, 108.1, 68.7, 35.4. HRMS (ESI) calcd

for C₁₇H₁₄ClNO [M+H]⁺ 284.0837, found 284.0842.

5.6.11 7-(3-Phenylpropoxy)-4-chloroquinoline (9k)

Starting from (3-bromopropyl)benzene (30 mmol), compound **9k** was isolated as a white solid (0.64 g, 54%), mp 51-52°. ESI-MS m/z [M+H]⁺ 297.9. ¹H NMR (300 MHz, CDCl₃): δ 8.64 (1H, d, *J* = 4.2 Hz, ArH), 8.08 (1H, d, *J* = 9.0 Hz, ArH), 7.36 (1H, s, ArH), 7.33-7.15 (7H, m, ArH), 4.10 (2H, t, *J* = 6.0 Hz, OCH₂CH₂CH₂), 2.84 (2H, t, *J* = 7.4 Hz, OCH₂CH₂CH₂), 2.26-2.10 (2H, m, OCH₂CH₂CH₂). ¹³C NMR (75 MHz, CDCl₃): δ 160.4 150.6, 149.8, 142.0, 140.9, 128.2(2C), 125.8, 124.9, 121.3, 120.7, 118.9, 108.0, 67.2, 32.1, 30.5. HRMS (ESI) calcd for C₁₈H₁₆ClNO [M+H]⁺ 298.0993, found 299.1011.

5.7 General procedure for compounds 10a-h

A mixture of 4-chloro-7-alkoxyquinoline **9** (2.0 mmol) and trimethyl orthoformate (53 g, 500 mmol) was heated under reflux for 2 h. After completion of the reaction as indicated by TLC, the solution was poured into H₂O (100 mL) and extracted with ethyl acetate. The organic phase was washed with water and brine and then dried over anhydrous sodium sulfate, filtered and evaporated. The resulting oil was purified by column chromatography using a mixture of dichloromethane and methanol 100:1 as the eluent to successfully afford the target products **10a-h** in good yield.

5.7.1 N-(2-(Dimethylamino)ethyl)-7-ethoxyquinolin-4-amine (10a)

Starting from 4-chloro-7-ethoxyquinoline **9a** (2.0 mmol) and N,N-diethylethylenediamine (4.0 mmol), a yellow solid (0.38 g, 74%) was obtained, mp 84-85°. ESI-MS m/z [M+H]⁺ 287.9. ¹H NMR (300 MHz, CDCl₃): δ 8.44 (1H, d,

$J = 5.1$ Hz, ArH), 7.61 (1H, d, $J = 9.0$ Hz, ArH), 7.28 (1H, s, ArH), 7.04 (1H, d, $J = 9.0$ Hz, ArH), 6.25 (1H, d, $J = 5.4$ Hz, ArH), 5.98 (1H, s, NH), 4.13 (2H, q, $J = 6.9$ Hz, OCH₂CH₃), 3.20 (2H, dd, $J = 10.2$ Hz, $J = 5.1$ Hz, HNCH₂CH₂), 2.75 (2H, t, $J = 5.7$ Hz, NHCH₂CH₂), 2.56 (4H, q, $J = 6.9$ Hz, N[CH₂CH₃]₂), 1.46 (3H, t, $J = 6.9$ Hz, OCH₂CH₃), 1.04 (6H, t, $J = 7.1$ Hz, N[CH₂CH₃]₂). ¹³C NMR (75 MHz, CDCl₃): δ 159.2, 151.1, 150.0, 149.7, 120.6, 116.9, 113.2, 108.5, 97.8, 63.3, 50.6, 46.4, 39.7, 14.7, 12.0. HRMS (ESI) calcd for C₁₇H₂₅N₃O [M+H]⁺ 288.2070, found 288.2078.

5.7.2 *N*-(3-(dimethylamino)propyl)-7-ethoxyquinolin-4-amine (10b)

Starting from 4-chloro-7-ethoxyquinoline **9a** (2.0 mmol) and 3-(diethylamino)propylamine (4.0 mmol), a yellow oil (0.41 g, 75%) was obtained. ESI-MS m/z [M+H]⁺ 302.1. ¹H NMR (400 MHz, CDCl₃): δ 8.41 (1H, d, $J = 5.4$ Hz, ArH), 7.83 (1H, s, NH), 7.64 (1H, d, $J = 9.0$ Hz, ArH), 7.30 (1H, s, ArH), 7.02 (1H, d, $J = 9.0$ Hz, ArH), 6.23 (1H, d, $J = 5.4$ Hz, ArH), 4.16 (2H, q, $J = 6.9$ Hz, CH₂CH₃), 3.38 (2H, d, $J = 4.5$ Hz, NCH₂CH₂CH₂), 2.65 (6H, dt, $J = 14.4$ Hz, $J = 6.0$ Hz, CH₂N[CH₂CH₃]₂), 1.97-1.83 (2H, m, NHCH₂CH₂CH₂), 1.47 (3H, t, $J = 6.8$ Hz, CH₂CH₃), 1.09 (6H, t, $J = 6.8$ Hz, N[CH₂CH₃]₂). ¹³C NMR (100 MHz, CDCl₃): δ 159.0, 150.5, 150.3, 149.5, 121.4, 116.0, 113.1, 107.8, 96.5, 62.9, 52.5, 46.4, 43.5. HRMS (ESI) calcd for C₁₈H₂₇N₃O [M+H]⁺ 302.2227, found 302.2223.

5.7.3 7-(Allyloxy)-*N*-(2-(dimethylamino)ethyl)quinolin-4-amine (10c)

Starting from 7-allyloxy-4-chloro-quinoline **9c** (2.0 mmol) and N,N-diethylethylenediamine (4.0 mmol), a yellow oil (0.43 g, 80%) was obtained. ESI-MS m/z [M+H]⁺ 300.1. ¹H NMR (300 MHz, CDCl₃): δ 8.43 (1H, d, $J = 5.4$ Hz,

ArH), 7.62 (1H, d, $J = 9.0$ Hz, ArH), 7.30 (1H, d, $J = 2.1$ Hz, ArH), 7.08 (1H, dd, $J = 9.3$ Hz, $J = 1.8$ Hz, ArH), 6.28 (1H, d, $J = 5.4$ Hz, ArH), 6.09 (1H, dd, $J = 15.9$ Hz, $J = 10.5$ Hz, $J = 5.1$ Hz, CH₂=CH), 5.97 (1H, s, NH), 5.46 (1H, d, $J = 17.2$ Hz, CH₂=CH), 5.31 (1H, d, $J = 10.5$ Hz, CH₂=CH), 4.65 (2H, d, $J = 5.1$ Hz, OCH₂CH=CH₂), 3.25 (2H, dd, $J = 10.5$ Hz, $J = 5.4$ Hz, NHCH₂CH₂), 2.80 (2H, t, $J = 5.7$ Hz, NHCH₂CH₂), 2.59 (4H, q, $J = 7.2$ Hz, [CH₂CH₃]₂), 1.07 (6H, t, $J = 7.2$ Hz, [CH₂CH₃]₂). ¹³C NMR (75 MHz, CDCl₃): δ 158.4, 150.4, 149.5, 149.3, 132.2, 120.8, 117.1, 116.3, 113.1, 108.2, 97.2, 68.1, 50.3, 46.0, 39.5, 11.4. HRMS (ESI) calcd for C₁₈H₂₅N₃O [M+H]⁺ 300.2070, found 300.2076.

5.7.4 7-(Allyloxy)-N-(3-(dimethylamino)propyl)quinolin-4-amine (10d)

Starting from 7-allyloxy-4-chloroquinoline **9c** (2.0 mmol) and 3-(diethylamino)propylamine (4.0 mmol), a yellow oil (0.18 g, 32%) was obtained. ESI-MS m/z [M+H]⁺ 313.9. ¹H NMR (300 MHz, CDCl₃): δ 8.40 (1H, d, $J = 5.4$ Hz, ArH), 7.83 (1H, s, NH), 7.64 (1H, d, $J = 9.0$ Hz, ArH), 7.03 (1H, dd, $J = 9.0$ Hz, $J = 1.5$ Hz, ArH), 6.20 (1H, d, $J = 5.4$ Hz, ArH), 6.08 (1H, ddd, $J = 21.6$ Hz, $J = 10.5$ Hz, $J = 5.1$ Hz, CH=CH₂), 5.45 (1H, d, $J = 17.2$ Hz, CH=CH₂), 5.29 (1H, d, $J = 10.5$ Hz, CH=CH₂), 4.63 (2H, d, $J = 5.1$ Hz, OCH₂CH=CH₂), 3.34 (2H, d, $J = 3.9$ Hz, NCH₂[CH₂]₂), 2.61 (6H, dd, $J = 13.8$ Hz, $J = 6.6$ Hz, CH₂N[CH₂CH₃]₂), 1.94-1.81 (m, 2H, NCH₂CH₂CH₂), 1.07 (6H, t, $J = 7.2$ Hz, N[CH₂CH₃]₂). ¹³C NMR (75 MHz, CDCl₃): δ 158.8, 151.0, 150.5, 149.8, 132.8, 121.7, 117.7, 116.5, 113.6, 108.7, 97.0, 68.7, 53.4, 47.0, 44.4, 24.5, 11.6. HRMS (ESI) calcd for C₁₉H₂₇N₃O [M+H]⁺ 314.2227, found 314.2232.

5.7.5 7-Hexyloxy-N-(3-(dimethylamino)ethyl)quinolin-4-amine (10e)

Starting from 4-chloro-7-(hexyloxy)quinoline **9f** (2.0 mmol) and N,N-diethylethylenediamine (4.0 mmol), a yellow solid (0.54 g, 85%) was obtained, mp 92-93 °C. ESI-MS m/z $[M+H]^+$ 344.0. 1H NMR (300 MHz, $CDCl_3$): δ 8.43 (1H, d, $J = 5.4$ Hz, ArH), 7.61 (1H, d, $J = 9.0$ Hz, ArH), 7.28 (1H, d, $J = 2.1$ Hz, ArH), 7.04 (1H, dd, $J = 9.0$ Hz, $J = 2.1$ Hz, ArH), 6.26 (1H, d, $J = 5.4$ Hz, ArH), 5.98 (1H, s, NH), 4.06 (2H, t, $J = 6.6$ Hz, $OCH_2[CH_2]_4CH_3$), 3.22 (2H, dd, $J = 10.2$ Hz, $J = 5.4$ Hz, $NHCH_2CH_2$), 2.77 (2H, t, $J = 5.8$ Hz, $NHCH_2CH_2$), 2.57 (4H, q, $J = 6.9$ Hz, $N[CH_2CH_3]_2$), 1.89-1.76 (2H, m, $OCH_2CH_2[CH_2]_3CH_3$), 1.54-1.42 (m, 2H, $O[CH_2]_2CH_2[CH_2]_2CH_3$), 1.34 (4H, d, $J = 3.6$ Hz, $O[CH_2]_3[CH_2]_2CH_3$), 1.05 (6H, t, $J = 7.2$ Hz, $N[CH_2CH_3]_2$), 0.90 (3H, t, $J = 6.6$ Hz, $O[CH_2]_5CH_3$). ^{13}C NMR (75 MHz, $CDCl_3$): δ 159.5, 151.1, 145.0, 149.8, 120.6, 117.1, 113.2, 108.6, 97.8, 68.0, 50.7, 46.5, 39.8, 31.6, 29.1, 25.8, 22.6, 14.1, 12.1. HRMS (ESI) calcd for $C_{21}H_{33}N_3O$ $[M+H]^+$ 344.2696, found 344.2707.

5.7.6 7-Benzoyloxy-N-(3-(dimethylamino)ethyl)quinolin-4-amine (10f)

Starting from 7-benzyloxy-4-chloro-quinoline **9h** (2.0 mmol) and N,N-diethylethylenediamine (4.0 mmol), a yellow solid (0.37 g, 58%) was obtained, mp 93-94 °C. ESI-MS m/z $[M+H]^+$ 349.9. 1H NMR (300 MHz, $CDCl_3$): δ 8.44 (1H, d, $J = 4.8$ Hz, ArH), 7.63 (1H, d, $J = 9.0$ Hz, ArH), 7.47 (2H, d, $J = 7.2$ Hz, ArH), 7.34 (4H, dd, $J = 13.5$ Hz, $J = 7.8$ Hz, ArH), 7.13 (1H, d, $J = 9.0$ Hz, ArH), 6.28 (1H, d, $J = 5.1$ Hz, ArH), 5.99 (1H, s, NH), 5.17 (2H, s, OCH_2Ph), 3.25 (2H, t, $J = 4.8$ Hz, $NHCH_2CH_2$), 2.80 (t, $J = 5.4$ Hz, 2H, $NHCH_2CH_2$), 2.59 (4H, q, $J = 6.9$ Hz, $N[CH_2CH_3]_2$), 1.07 (6H, t, $J = 6.9$ Hz, $N[CH_2CH_3]_2$). ^{13}C NMR (75 MHz, $CDCl_3$): δ 159.1, 151.1, 149.9, 136.5,

128.4, 127.9, 127.5, 120.9, 117.1, 113.6, 109.6, 109.2, 105.2, 98.0, 70.0, 50.8, 46.5, 39.8, 12.1. HRMS (ESI) calcd for C₂₂H₂₇N₃O [M+H]⁺ 350.2227, found 350.2232.

5.7.7 7-(4-Fluorobenzyloxy)-N-(2-(dimethylamino)ethyl)quinolin-4-amine (10g)

Starting from 7-(4-fluorobenzyloxy)-4-chloro-quinoline **9i** (2.0 mmol) and N,N-diethylethylenediamine (4.0 mmol), a white solid (0.38 g, 56%) was obtained, mp 67-68 °C. ESI-MS m/z [M+H]⁺ 367.7. ¹H NMR (300 MHz, CDCl₃): δ 8.44 (1H, d, *J* = 5.4 Hz, ArH), 7.63 (1H, d, *J* = 9.0 Hz, ArH), 7.42 (2H, dd, *J* = 8.4 Hz, *J* = 5.4 Hz, ArH), 7.36 (1H, d, *J* = 2.4 Hz, ArH), 7.10 (1H, dd, *J* = 9.0 Hz, *J* = 2.4 Hz, ArH), 7.04 (2H, t, *J* = 8.7 Hz, ArH), 6.27 (1H, d, *J* = 5.4 Hz, ArH), 5.99 (1H, d, *J* = 2.4 Hz, NH), 5.11 (2H, s, OCH₂Ph[p-F]), 3.23 (2H, dd, *J* = 10.5 Hz, *J* = 5.4 Hz, NHCH₂CH₂), 2.78 (2H, t, *J* = 6.0 Hz, NHCH₂CH₂), 2.58 (4H, q, *J* = 7.2 Hz, N[CH₂CH₃]₂), 1.06 (6H, t, *J* = 7.2 Hz, N[CH₂CH₃]₂). ¹³C NMR (75 MHz, CDCl₃): δ 162.32 (d, *J* = 246.0 Hz), 159.0, 151.0, 149.9, 149.8, 132.3, 129.32 (d, *J* = 7.9 Hz), 121.0, 117.0, 115.33 (d, *J* = 21.5 Hz), 113.6, 109.1, 98.0, 69.3, 50.8, 46.6, 39.9, 12.1. HRMS (ESI) calcd for C₂₂H₂₆FN₃O [M+H]⁺ 368.2133, found 368.2139.

5.7.8 7-(4-Fluorobenzyloxy)-N-(3-(dimethylamino)propyl)quinolin-4-amine (10h)

Starting from 7-(4-fluorobenzyloxy)-4-chloro-quinoline **9i** (2.0 mmol) and 3-(diethylamino)propylamine (4.0 mmol), a yellow oil (0.48 g, 68%) was obtained. ESI-MS m/z [M+H]⁺ 382.4. ¹H NMR (300 MHz, CDCl₃): δ 8.41 (1H, d, *J* = 5.1 Hz, ArH), 7.83 (1H, s, NH), 7.66 (1H, d, *J* = 9.0 Hz, ArH), 7.45-7.36 (2H, m, ArH), 7.34 (1H, s, ArH), 7.13-6.95 (3H, m, ArH), 6.20 (1H, d, *J* = 5.1 Hz, ArH), 5.08 (2H, s, OCH₂Ph[p-F]), 3.32 (2H, s, NHCH₂(CH₂)₂), 2.67-2.53 (6H, m, CH₂N[CH₂CH₃]₂),

1.84 (2H, s, NHCH₂CH₂CH₂), 1.06 (6H, t, $J = 6.9$ Hz, N[CH₂CH₃]₂). ¹³C NMR (75 MHz, CDCl₃): δ 162.0 (d, $J = 245.7$ Hz), 158.6, 151.0, 150.3, 149.7, 132.11 (d, $J = 2.0$ Hz), 129.0 (d, $J = 8.0$ Hz), 121.7, 116.1, 115.0 (d, $J = 21.4$ Hz), 113.6, 108.8, 96.8, 68.9, 53.0, 46.7, 44.1, 24.3, 11.4. HRMS (ESI) calcd for C₂₃H₂₈FN₃O [M+H]⁺ 382.2289, found 382.2298.

5.8 Cell lines and cell culture

The human cancer cells (HCT116, RKO, DLD1, HepG2, BGC-823, NCI-H1650 and SK-OV-3) were purchase from American Type Culture Collection (ATCC, Rockville, MD). HCT116 *p53*^{-/-} and HCT116 *Bax*^{-/-} cell lines were kindly provided by Dr. Bert Vogelstein (The Sidney Kimmel Comprehensive Cancer Center, The Johns Hopkins University Medical Institutions, Baltimore). All cells were cultured in McCoy's 5A medium (AppliChem) supplemented with 10% fetal bovine serum (HyClone, Logan, UT, USA), 100 units·mL⁻¹ streptomycin and 100 units·mL⁻¹ penicillin at 37°C in a humidified atmosphere of 5% CO₂ and 95% air.

5.9 Cytotoxicity in vitro

Cell proliferative assay were carried out using 96 microtitre plate cultures and MTT staining. Cells were grown in RPMI-1640 medium containing 10% (v/v) fetal calf serum and 100 μ M penicillin and 100 μ M streptomycin. Cultures were propagated at 37°C in a humified atmosphere containing 5% CO₂, Cells in logarithmic phase were diluted to a density of 50,000 cells/mL in culture medium and treated with various concentrations of compounds **9a-k** and **10a-h** in 96-well plates for 48 h in final volumes of 200 μ L. Then 20 μ L MTT (5 mg/mL) was added to each well, and

the cells were incubated for additional 4 h. After carefully removing the medium, the precipitates were dissolved in 200 μ L of DMSO, shaken mechanically for 2 min, and then absorbance values at a wavelength of 570 nm were taken on a spectrophotometer (Bio-Rad iMark microplate absorbance Reader, USA). IC₅₀ values were calculated using percentage of growth versus untreated control. Cisplatin and 7-chloro-4(1H)-quinolone **11** were used as positive controls and DMSO was used as the solution for drugs. Final concentration of DMSO in the growth medium was 2% (v/v) or lower, concentration without effect on cell replication. In all of these experiments, three replicate wells were used to determine each point.

5.10 Cell viability assay

Cells were seeded into 96-well plates at a density of 2×10^4 per well, cultured for 24 h, and then treated with increasing doses of the tested compounds **7**, **9a-k** and **10a-h** for 48 h. Cell viability was assayed using Cell Counting Kit-8 (CCK-8, Dojindo Laboratories, Kumamoto, Japan) following the manufacturer's protocol. The concentration required to inhibit cell growth by 50% (IC₅₀) was calculated from viability curves as previously reported.

5.11 Colony formation assay

The indicated cells were counted and seeded in 12-well plates for colony formation assays. Cells were cultured overnight, and then, the medium was replaced with medium containing compound **10g** at the indicated concentration. After 24 h of exposure, the medium was changed back to standard culture medium, and the cells were cultured for 9-10 days. The colonies were dyed with 1% crystal violet dye

containing 4% paraformaldehyde for 30 min and washed with water. The colonies were then photographed and counted using ImageJ software.

5.12 Apoptosis and cell cycle assay

Apoptotic cells were quantitated using an Annexin V-FITC apoptosis detection kit after treatment with compound **10g** at 0, 2.5 and 5 μ M for 24 h. To investigate the mechanisms by which compound **10g** induces apoptosis, cells were pretreated with 20 μ M z-VAD-FMK for 12 h and then treated with 2.5 μ M or 5 μ M compound **10g** for an additional 24 h. Following treatment, the cells were trypsinized, washed twice with cold PBS and resuspended in 100 μ l of binding buffer. Then, Annexin V-FITC and PI were added to the cells. After incubation for 15 min at 37 $^{\circ}$ C in the dark, an additional 400 μ l of binding buffer was added to the cells, and they were then subjected to FACS cytometry. The results were analyzed with Summit 4.3 software. For cell cycle analysis, the cells were fixed in 70% ice-cold ethanol, incubated at 4 $^{\circ}$ C for 1 h, and then centrifuged at 1000 g for 5-10 min. The cell pellet was washed and suspended in 0.5 mL of PBS containing 50 μ g/mL RNase A at 37 $^{\circ}$ C for 30 min. Then, 50 μ g/mL PI solution was added and incubated with cells for another 30 min at room temperature in the dark. The cells were analyzed via flow cytometry to assess cell cycle distribution.

5.13 Autophagy and ROS assays

The GFP-LC3 cell line was used to examine autophagy. GFP puncta were observed using a fluorescence microscope and counted after exposure to the indicated concentration of compound **10g** for 12 h. For the ROS assay, cells were exposed to

the indicated concentration of compound **10g** and then stained with DCFH-DA followed by FACS analysis.

5.14 Immunoblotting analysis

Cells were treated with compound **10g** at the indicated concentration for 0-24 h and harvested at 80% confluence. Then, the cells were lysed with SDS sample buffer and boiled for 5-10 min. Protein concentration was determined with a BCA protein assay kit (Thermo), and 20 µg samples were loaded into SDS-PAGE gels. Proteins were transferred to polyvinylidene difluoride (PVDF) membranes, which were then blocked with TBST containing 5% dry fat milk and incubated with primary antibodies overnight at 4°C, followed by incubation with HRP-conjugated secondary antibody for 1 h at room temperature. Then, the immunoblots were visualized with an Immobilon Western Chemiluminescent HRP Substrate kit (Merck Millipore).

5.15 Xenograft tumor model

To further examine the anticancer role of compound **10g** *in vivo*, we established a human colorectal cancer xenograft model in 6-week-old male C57 mice by subcutaneously injecting CT26-CL25 cells (3×10^6) into the flanks of the mice. The mice were randomly divided into two groups, a vehicle control group and a compound **10g** treatment group, when the tumor grew to 3-5 mm in diameter. Compound **10g** (80 mg/kg body weight) was administered once every three days for 21 days. The tumors were photographed, and tumor weights were obtained on day 21.

5.16 Statistical analysis

The data given in the text were expressed as means \pm SD. The significance of

the difference between compared groups was determined with the Student's t test. The differences were considered significant at * $p < 0.05$ and ** $p < 0.01$.

5.17 Ethics statement

All of the animal studies were conducted in accordance with the Guidelines of China Animal Welfare Legislation, as proved by the Committee on Ethics in the Care and Use of Laboratory Animals of Sun Yat-sen University. All efforts were made to minimize suffering.

Acknowledgments

This work was supported by grants from the Natural Science Foundation of Guangdong Province [S2013010012138 and 2016A030313349] and the Fundamental Research Funds for the Central Universities [413000099] and Zhongnan Hospital of Wuhan University Science, Technology and Innovation Seed Fund Project [cxy2017005].

References

- [1] J.A. Call, S.G. Eckhardt, D.R. Camidge, Targeted manipulation of apoptosis in cancer treatment, *Lancet Oncology* 9 (2008) 1002-1011.
- [2] A. Ali, M.Z. Bhatti, A.S. Shah, H.Q. Duong, H.M. Alkreathy, S.F. Mohammad, R.A. Khan, A. Ahmad, Tumor-suppressive p53 Signaling Empowers Metastatic Inhibitor KLF17-dependent Transcription to Overcome Tumorigenesis in Non-small Cell Lung Cancer, *Journal of Biological Chemistry* 290 (2015) 21336-21351.
- [3] V. Marcel, F.N. Van Long, J.J. Diaz, 40 Years of Research Put p53 in Translation, *Cancers* 10 (2018).
- [4] K.C. Fang, Y.L. Chen, J.Y. Sheu, T.C. Wang, C.C. Tzeng, Synthesis, antibacterial, and cytotoxic evaluation of certain 7-substituted norfloxacin derivatives, *Journal of Medicinal Chemistry* 43 (2000) 3809-3812.
- [5] D. Verbanac, R. Malik, M. Chand, K. Kushwaha, M. Vashist, M. Matijasic, V. Stepanic, M. Peric, H.C. Paljetak, L. Saso, S.C. Jain, Synthesis and evaluation of antibacterial and antioxidant activity of

- novel 2-phenyl-quinoline analogs derivatized at position 4 with aromatically substituted 4H-1,2,4-triazoles, *Journal of Enzyme Inhibition and Medicinal Chemistry* 31 (2016) 104-110.
- [6] Q. Li, J.H. Xing, H.B. Cheng, H. Wang, J. Wang, S. Wang, J.P. Zhou, H.B. Zhang, Design, Synthesis, Antibacterial Evaluation and Docking Study of Novel 2-Hydroxy-3-(nitroimidazolyl)-propyl-derived Quinolone, *Chemical Biology & Drug Design* 85 (2015) 79-90.
- [7] Salahuddin, A. Mazumder, M. Shaharyar, Synthesis, antibacterial and anticancer evaluation of 5-substituted (1,3,4-oxadiazol-2-yl)quinoline, *Medicinal Chemistry Research* 24 (2015) 2514-2528.
- [8] C. Shen, J. Xu, C.C. Xia, Y. Yang, H.Y. Shen, B.B. Ying, X.L. Zhu, P.F. Zhang, 4-quinolone derivatives: Synthesis and antitumor activity, *Science* 360 (2018) 20-23.
- [9] L. Pintilie, A. Stefaniu, A.I. Nicu, M.T. Caproiu, M. Maganu, Synthesis, Antimicrobial Activity and Docking Studies of Novel 8-Chloro-quinolones, *Revista De Chimie* 67 (2016) 438-445.
- [10] B. Natalini, R. Sardella, S. Massari, F. Ianni, O. Tabarrini, V. Cecchetti, Synthesis and chromatographic enantioresolution of anti-HIV quinolone derivatives, *Talanta* 85 (2011) 1392-1397.
- [11] P. Sridhar, M. Alagumuthu, S. Arumugam, S.R. Reddy, Synthesis of quinoline acetohydrazone-derivative derivatives evaluated as DNA gyrase inhibitors and potent antimicrobial agents, *Rsc Advances* 6 (2016) 64460-64468.
- [12] C.H. Song, H.W. Ryu, J.K. Park, T.S. Ko, Mechanism of DNA gyrase inhibition by quinolones: I. Spectral analysis for nalidixic acid polymorphism, *Bulletin of the Korean Chemical Society* 20 (1999) 727-730.
- [13] K.J. Aldred, S.A. McPherson, P.F. Wang, R.J. Kerns, D.E. Graves, C.L. Turnbough, N. Osheroff, Drug Interactions with *Bacillus anthracis* Topoisomerase IV: Biochemical Basis for Quinolone Action and Resistance, *Biochemistry* 51 (2012) 370-381.
- [14] K. Li, Y. Li, D. Zhou, Y.B. Fan, H.Y. Guo, T.Y. Ma, J.C. Wen, D. Liu, L.X. Zhao, Synthesis and biological evaluation of quinoline derivatives as potential anti-prostate cancer agents and Pim-1 kinase inhibitors, *Bioorganic & Medicinal Chemistry* 24 (2016) 1889-1897.
- [15] K. Abouzid, S. Shouman, Design, synthesis and in vitro antitumor activity of 4-aminoquinoline and 4-aminoquinazoline derivatives targeting EGFR tyrosine kinase, *Bioorganic & Medicinal Chemistry* 16 (2008) 7543-7551.
- [16] X.Q. Wang, N. Jiang, S.J. Zhao, S.C. Xi, J. Wang, T.F. Jing, W.Y. Zhang, M. Guo, P. Gong, X. Zhai, Design, synthesis and biological evaluation of novel 4-(2-fluorophenoxy) quinoline derivatives as selective c-Met inhibitors, *Bioorganic & Medicinal Chemistry* 25 (2017) 886-896.
- [17] A.G. Shilabin, L. Dzhekieva, P. Misra, B. Jayaram, R.F. Pratt, 4-Quinolones as Noncovalent Inhibitors of High Molecular Mass Penicillin-Binding Proteins, *Acs Medicinal Chemistry Letters* 3 (2012) 592-595.
- [18] L. Wang, X.B. Hou, H.S. Fu, X.L. Pan, W.F. Xu, W.P. Tang, H. Fang, Design, synthesis and preliminary bioactivity evaluations of substituted quinoline hydroxamic acid derivatives as novel histone deacetylase (HDAC) inhibitors, *Bioorganic & Medicinal Chemistry* 23 (2015) 4364-4374.
- [19] S.K. Srivastava, A. Jha, S.K. Agarwal, R. Mukherjee, A.C. Burman, Synthesis and structure-activity relationships of potent antitumor active quinoline and naphthyridine derivatives, *Anti-Cancer Agents in Medicinal Chemistry* 7 (2007) 685-709.
- [20] J. Sun, H. Zhu, Z.M. Yang, H.L. Zhu, Synthesis, molecular modeling and biological evaluation of 2-aminomethyl-5-(quinolin-2-yl)-1,3,4-oxadiazole-2(3H)-thione quinolone derivatives as novel anticancer agent, *European Journal of Medicinal Chemistry* 60 (2013) 23-28.

- [21] O. Afzal, S. Kumar, M.R. Haider, M.R. Ali, R. Kumar, M. Jaggi, S. Bawa, A review on anticancer potential of bioactive heterocycle quinoline, *European Journal of Medicinal Chemistry* 97 (2015) 871-910.
- [22] A.R. Kumar, B.P.V. Lingaiah, P.S. Rao, B. Narsaiah, D. Sriram, P. Sowjanya, Synthesis and biological evaluation of novel N1-decyl and C7-sec amine substituted fluoroquinolones as antitubercular and anticancer agents, *Indian Journal of Chemistry Section B-Organic Chemistry Including Medicinal Chemistry* 54 (2015) 1495-1501.
- [23] V.V. Kouznetsov, F. Sojo, F.A. Rojas-Ruiz, D.R. Merchan-Arenas, F. Arvelo, Synthesis and cytotoxic evaluation of 7-chloro-4-phenoxyquinolines with formyl, oxime and thiosemicarbazone scaffolds, *Medicinal Chemistry Research* 25 (2016) 2718-2727.
- [24] K.R.A. Abdellatif, E.K.A. Abdelall, M.A. Abdelgawad, D.M.E. Amin, H.A. Omar, Design, synthesis and biological evaluation of new 4-(4-substituted-anilino)quinoline derivatives as anticancer agents, *Medicinal Chemistry Research* 26 (2017) 929-939.
- [25] I. Khelifi, T. Naret, D. Renko, A. Hamze, G. Bernadat, J. Bignon, C. Lenoir, J. Dubois, J.D. Brion, O. Provot, M. Alami, Design, synthesis and anticancer properties of IsoCombretaQuinolines as potent tubulin assembly inhibitors, *European Journal of Medicinal Chemistry* 127 (2017) 1025-1034.
- [26] K. Marciniak, B. Pawelczak, M. Latocha, L. Skrzypek, M. Maciazek-Jurczyk, S. Boryczka, Synthesis, Anti-Breast Cancer Activity, and Molecular Docking Study of a New Group of Acetylenic Quinolinesulfonamide Derivatives, *Molecules* 22 (2017).
- [27] Q. Chen, W. Geng, Antiume, *Chinese Journal of New Drugs* 14 (2005) 1231-1232.
- [28] Z.Y. Zhang, X.P. Xiao, T. Su, J.Y. Wu, J.W. Ren, J.C. Zhu, X.D. Zhang, R.H. Cao, R.L. Du, Synthesis, structure-activity relationships and preliminary mechanism of action of novel water-soluble 4-quinolone-3-carboxamides as antiproliferative agents, *European Journal of Medicinal Chemistry* 140 (2017) 239-251.
- [29] C.C. Price, R.M. Roberts, The synthesis of 4-hydroxyquinolones. I. Through ethoxymethylenemalonic ester, *J. Am. Chem. Soc.* 68 (1946) 1204-1208.
- [30] R.H. Cao, W.X. Fan, L. Guo, Q. Ma, G.X. Zhang, J.R. Li, X.M. Chen, Z.H. Ren, L.Q. Qiu, Synthesis and structure-activity relationships of harmine derivatives as potential antitumor agents, *European Journal of Medicinal Chemistry* 60 (2013) 135-143.
- [31] C.M. Ma, R.H. Cao, B.X. Shi, X.T. Zhou, Q. Ma, J. Sun, L.A. Guo, W. Yi, Z.Y. Chen, H.C. Song, Synthesis and cytotoxic evaluation of 1-carboxamide and 1-amino side chain substituted beta-carbolines, *European Journal of Medicinal Chemistry* 45 (2010) 5513-5519.
- [32] Z.Y. Chen, R.H. Cao, B.X. Shi, L. Guo, J. Sun, Q. Ma, W.X. Fan, H.C. Song, Synthesis and biological evaluation of 1,9-disubstituted beta-carbolines as potent DNA intercalating and cytotoxic agents, *European Journal of Medicinal Chemistry* 46 (2011) 5127-5137.
- [33] Z.Y. Chen, R.H. Cao, B.X. Shi, W. Yi, L.A. Yu, H.C. Song, Z.H. Ren, W.L. Peng, Synthesis of novel beta-carbolines with efficient DNA-binding capacity and potent cytotoxicity, *Bioorganic & Medicinal Chemistry Letters* 20 (2010) 3876-3879.
- [34] Z.Y. Chen, R.H. Cao, L.A. Yu, B.X. Shi, J. Sun, L.A. Guo, Q. Ma, W. Yi, X.A. Song, H.C. Song, Synthesis, cytotoxic activities and DNA binding properties of beta-carboline derivatives, *European Journal of Medicinal Chemistry* 45 (2010) 4740-4745.
- [35] C.T. Chang, M. Korivi, H.C. Huang, V. Thiyagarajan, K.Y. Lin, P.J. Huang, J.Y. Liu, Y.C. Hseu, H.L. Yang, Inhibition of ROS production, autophagy or apoptosis signaling reversed the anticancer properties of *Antrodia salmonea* in triple-negative breast cancer (MDA-MB-231) cells, *Food and*

Chemical Toxicology 103 (2017) 1-17.

[36] S. Yu, L.J. Wang, Z.X. Cao, D.Y. Gong, Q.Y. Liang, H.T. Chen, H.Z. Fu, W.W. Wang, X. Tang, Z.H. Xie, Y. He, C. Peng, Y.Z. Li, Anticancer effect of Polyphyllin in colorectal cancer cells through ROS-dependent autophagy and G2/M arrest mechanisms, *Natural Product Research* 32 (2018) 1489-1492.

[37] J. Bai, Y. Li, G.X. Zhang, Cell cycle regulation and anticancer drug discovery, *Cancer Biology and Medicine* 14 (2017) 248-362.

[38] K. Katsumata, T. Sumi, H. Tomioka, T. Aoki, Y. Koyanagi, Induction of apoptosis by p53, bax, bcl-2, and p21 expressed in colorectal cancer, *International Journal of Clinical Oncology* 8 (2003) 352-356.

[39] J. Ye, J. Li, X. Wang, L. Li, Medicinal supplement genipin induces p53 and Bax-dependent apoptosis in colon cancer cells, *Oncology Letters* 16 (2018) 2957-2964.

[40] C. Castrogiovanni, B. Waterschoot, O. De Backer, P. Dumont, Serine 392 phosphorylation modulates p53 mitochondrial translocation and transcription-independent apoptosis, *Cell Death and Differentiation* 25 (2018) 190-203.

[41] I. Kaminska, J.K. Bar, The association between p53 protein phosphorylation at serine 15, serine 20 and sensitivity of cells isolated from patients with ovarian cancer and cell lines to chemotherapy in in vitro study, *Pharmacological Reports* 70 (2018) 570-576.

[42] I. Lopez, P.O.L. Tucci, P. , F. Alvarez-Valin, A.C.R. Marin, M., Different mutation profiles associated to P53 accumulation in colorectal cancer, *Gene* 499 (2012) 81-87.

[43] A. Nasierowska-Guttmejer, L. Trzeciak, M.P. Nowacki, J. Ostrowski, p53 protein accumulation and p53 gene mutation in colorectal cancer, *Pathology and Oncology Research* 6 (2000) 275-279.

[44] K.M. Webley, A.J. Shorthouse, J.A. Royds, Effect of mutation and conformation on the function of p53 in colorectal cancer, *Journal of Pathology* 191 (2000) 361-367.

[45] J.L. Coll, A. Negoescu, N. Louis, L. Sachs, C. Tenaud, V. Girardot, B. Demeinex, E. Brambilla, C. Brambilla, M. Favrot, Antitumor activity of bax and p53 naked gene transfer in lung cancer: in vitro and in vivo analysis, *Human Gene Therapy* 9 (1998) 2063-2074.

[46] P. Haghghat, T.M. Timiryasova, B. Chen, E.H. Kajioka, D.S. Gridley, I. Fodor, Antitumor effect of IL-2, p53, and bax gene transfer in C6 glioma cells, *Anticancer Research* 20 (2000) 1337-1342.

[47] S. Kagawa, J. Gu, S.G. Swisher, L. Ji, J.A. Roth, D. Lai, L.C. Stephens, B. Fang, Antitumor effect of adenovirus-mediated Bax gene transfer on p53-sensitive and p53-resistant cancer lines, *Cancer Research* 60 (2000) 1157-1161.

Legends

Tables

Table 1 *In vitro* cytotoxic activity of quinolone derivatives^c (IC₅₀, μM^a)

^aThe cytotoxicity for each cell line is shown by the IC₅₀, the concentration of compound that reduced the optical density of treated cells by 50% relative to that of untreated cells in an MTT assay.

^bThe cell lines tested were human laryngeal carcinoma (HCT-116, RKO and DLD1), liver carcinoma (HepG2), gastric carcinoma (BGC-823), non-small-cell lung carcinoma (NCI-H1650) and ovarian carcinoma (SK-OV-3) cell lines.

^cThe data represent the mean values of three independent determinations.

Figures

Fig. 1 The chemical structure of the lead compound 7-chloro-4(1H)-quinolone.

Fig. 2 Compound **10g** inhibited the viability of human colorectal cancer cells.

(A) Cells were treated with 5 μM compound **10g** for 24 h, and then, the drug was withdrawn; cell viability was determined at the indicated time. (B) The inhibition effect of compound **10g** on colony formation was evaluated in the three colorectal cancer cell lines. Colonies were stained with crystal violet dye and photographed. (C) The effect of compound **10g** on cell growth was monitored by micrographs. HCT116, DLD1 and RKO cells were exposed to compound **10g** at the indicated concentration for 24 h, and cell morphology was observed with a microscope. (D and E) The susceptibility of normal human colorectal and hepatic cell lines and cancer cell lines to compound **10g**. The normal colorectal and hepatic cell lines and cancer cell lines were exposed to the indicated concentration of compound **10g** for 24 h, and the cell viability was measured with a CCK8 assay.

Fig. 3 Compound **10g** induced cell apoptosis in HCT-116 cells.

(A) Flow cytometry analysis of compound **10g** induced apoptosis. HCT116 cells were treated with 5 μM or 10 μM compound **10g** for 24 h, stained with Annexin V/PI and then subjected to flow cytometry analysis. (B) A caspase inhibitor rescued compound **10g** induced apoptosis. The cells were pretreated with 20 μM z-VAD-FMK for 12 h, and then, compound **10g** was added for 24 h, followed by flow cytometry analysis. (C) HCT116 cells were treated with 2.5, 5 or 10 μM compound **10g** for 24 h and then subjected to an immunoblotting assay using the indicated antibodies. GAPDH was used as the loading control. (D) The cells were pretreated with 20 μM z-VAD-FMK for 12 h and then exposed to compound **10g** for 24 h, followed by an immunoblotting assay using a cleaved PARP antibody. GAPDH was used as the loading control.

Fig. 4 Compound **10g** induced apoptosis is independent of ROS and autophagy.

(A) Assessment of autophagy induced by compound **10g** via observation of GFP-LC3 puncta. HCT116 cells were treated with the indicated concentration of compound **10g** for 24 h, and photos were obtained with a fluorescence microscope. (B) The effect of compound **10g** on ROS production. HCT116 cells were treated with 5 μ M or 10 μ M compound **10g** or the positive control for 24 h, stained with DCFH-DA and then subjected to flow cytometry analysis. (C and D) The effect of compound **10g** on cell cycle arrest. HCT116 cells were treated with the indicated concentration of compound **10g**, stained with PI and then subjected to flow cytometry analysis.

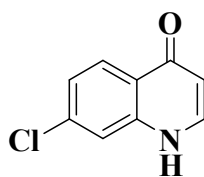
Fig. 5 Compound **10g** induced apoptosis by activating p53 transcriptional activity.

(A) CCK8 assays were used to analyze the viability of HCT116, p53^{-/-} and Bax^{-/-} cell lines. (B) Colony formation assays were used to analyze the viability of HCT116, p53^{-/-} and Bax^{-/-} cell lines. (C) Flow cytometry was used to analyze apoptosis induced by 5 μ M compound **10g** in HCT116, p53^{-/-} and Bax^{-/-} cell lines. (D) PARP and p53 target genes were analyzed with an immunoblotting assay. HCT116 and HCT116 p53^{-/-} cell lines were treated with the indicated concentration of compound **10g** for 24 h. The levels of apoptosis-associated proteins were detected by western blotting analysis using the indicated antibodies. GAPDH was used as the loading control. (E) The phosphorylation level of p53 induced by compound **10g** was measured with an immunoblotting assay. The phosphorylation of Ser15 and Ser329 in p53 was detected by western blotting analysis using the indicated antibodies. GAPDH was used as the loading control. (F) compound **10g** induced p53 translocation from the cytosol to the nucleus. HCT116 cells were treated with compound **10g** for the indicated time, and nuclear and cytosolic fractions were isolated. p53 was detected with an immunoblotting assay. Lamin A/C and Tubulin were used as the loading controls for the nuclear and cytosolic fractions, respectively.

Fig. 6 Compound **10g** inhibited tumor growth *in vivo*

HCT116 cells were injected into mice to establish an *in vivo* tumor model according to the instructions in the Materials and Methods. The tumors were removed from mice after 21 days growth, and the removed tumors were weighed and statistically analyzed (n=6). The data are presented as the means \pm SDs.

Fig. 1 The chemical structure of the lead compound 7-chloro-4(1H)-quinolone.



11

ACCEPTED MANUSCRIPT

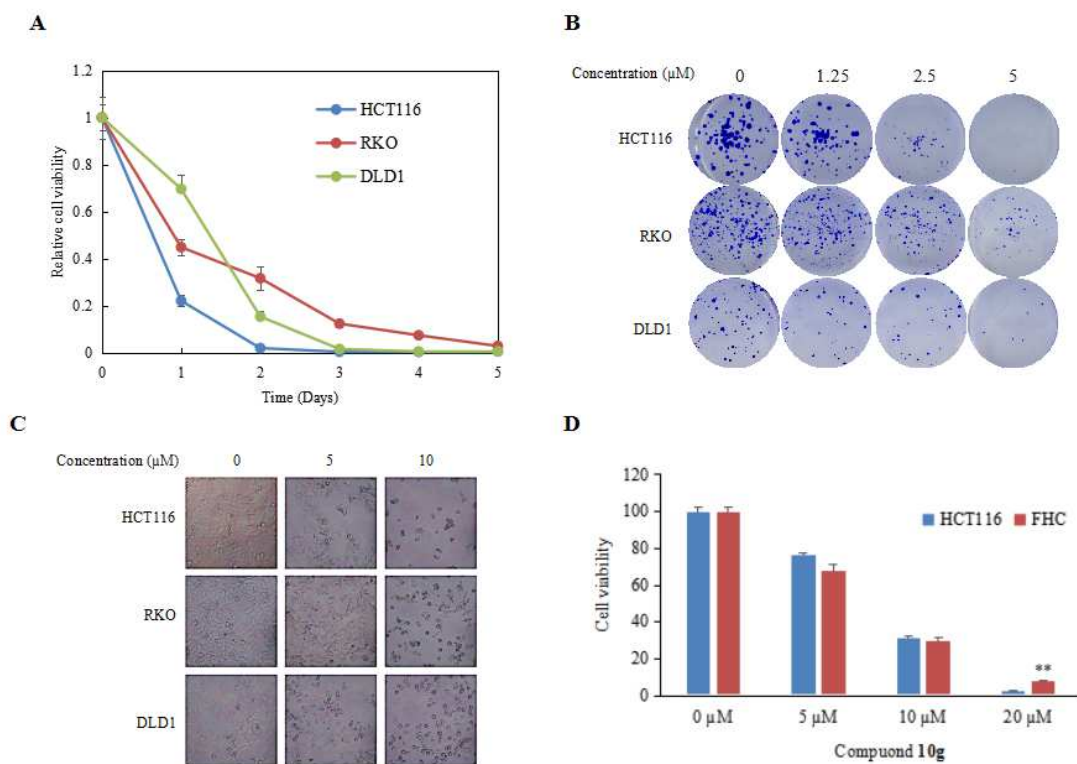
Fig. 2 Compound **10g** inhibited viability of human colorectal cancer cells.

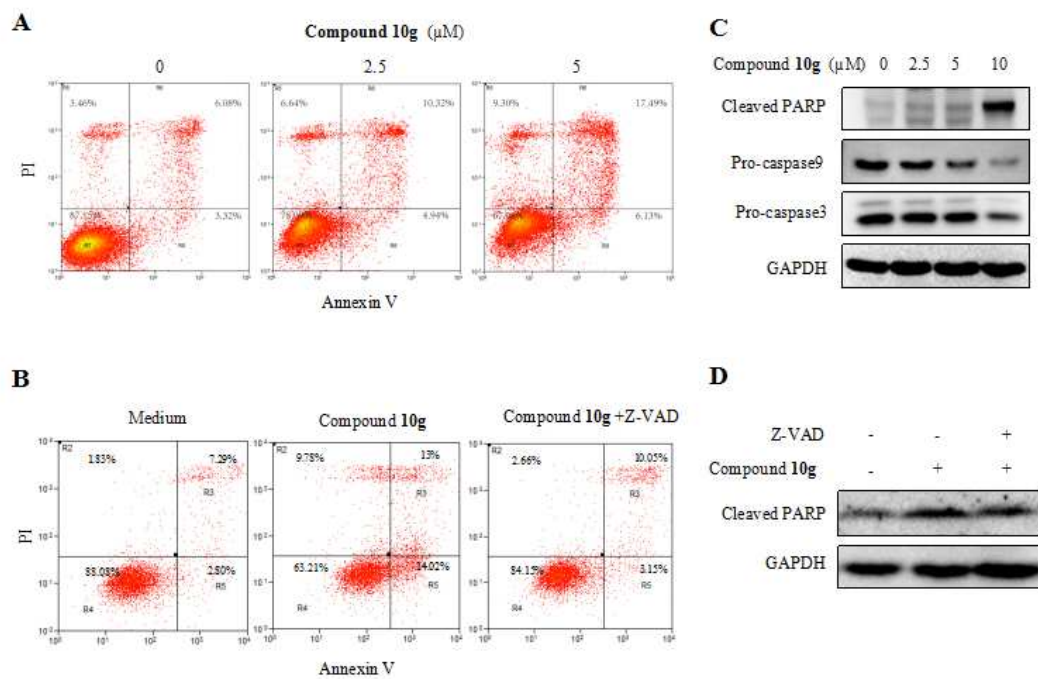
Fig. 3 Compound 10g induced cell apoptosis in HCT-116.

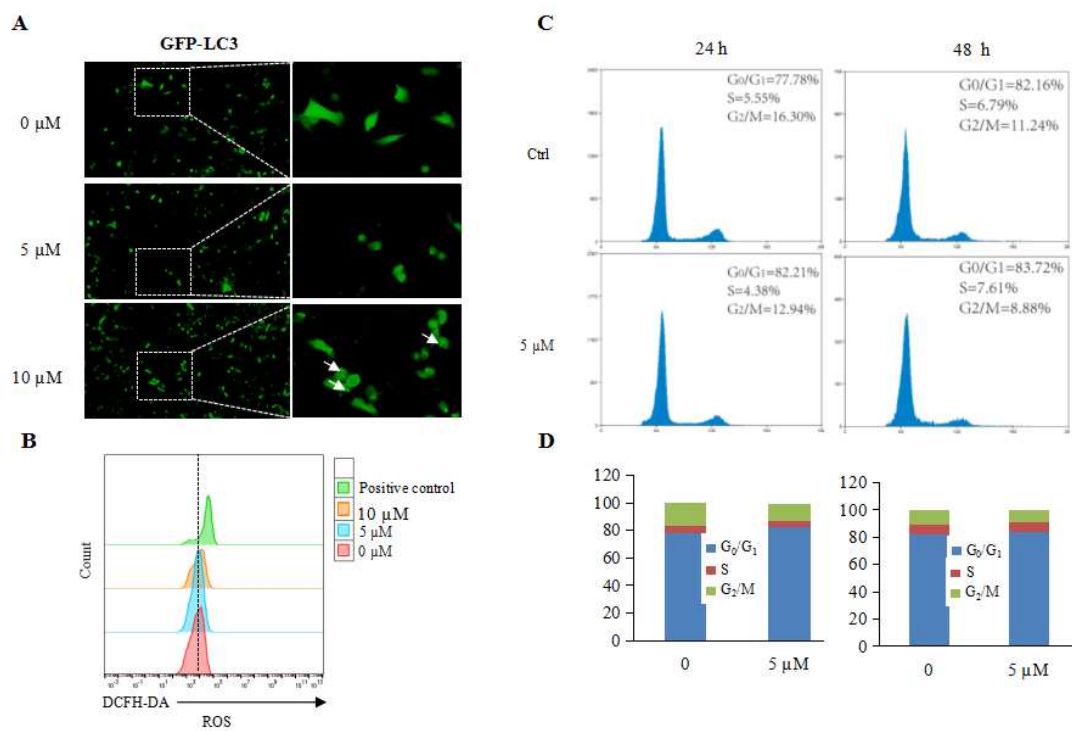
Fig. 4 Compound **10g** induced apoptosis is independent on ROS accumulation and autophagy.

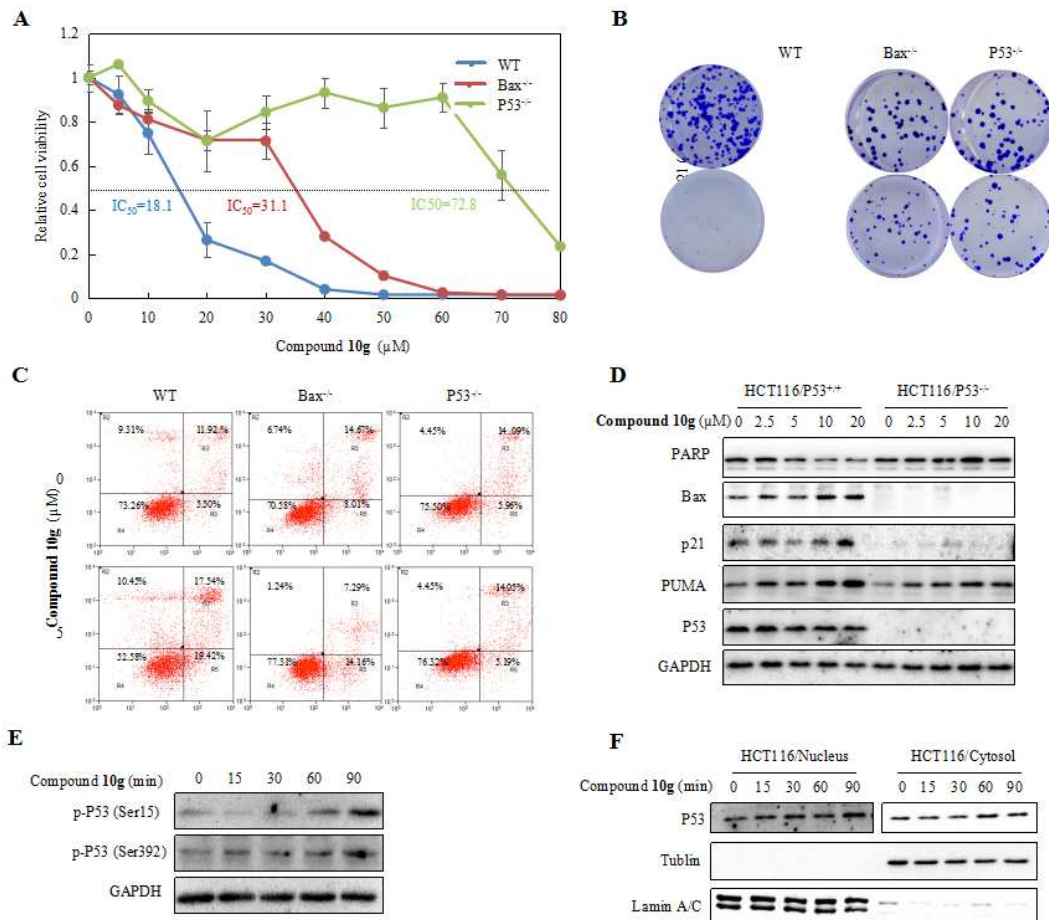
Fig. 5 Compound **10g** induced apoptosis via activating p53 transcriptional activity.

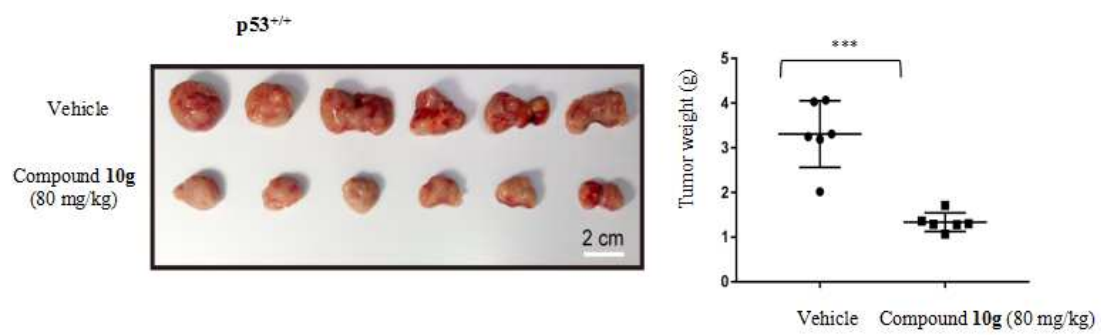
Fig. 6 Compound 10g inhibited tumor growth *in vivo*

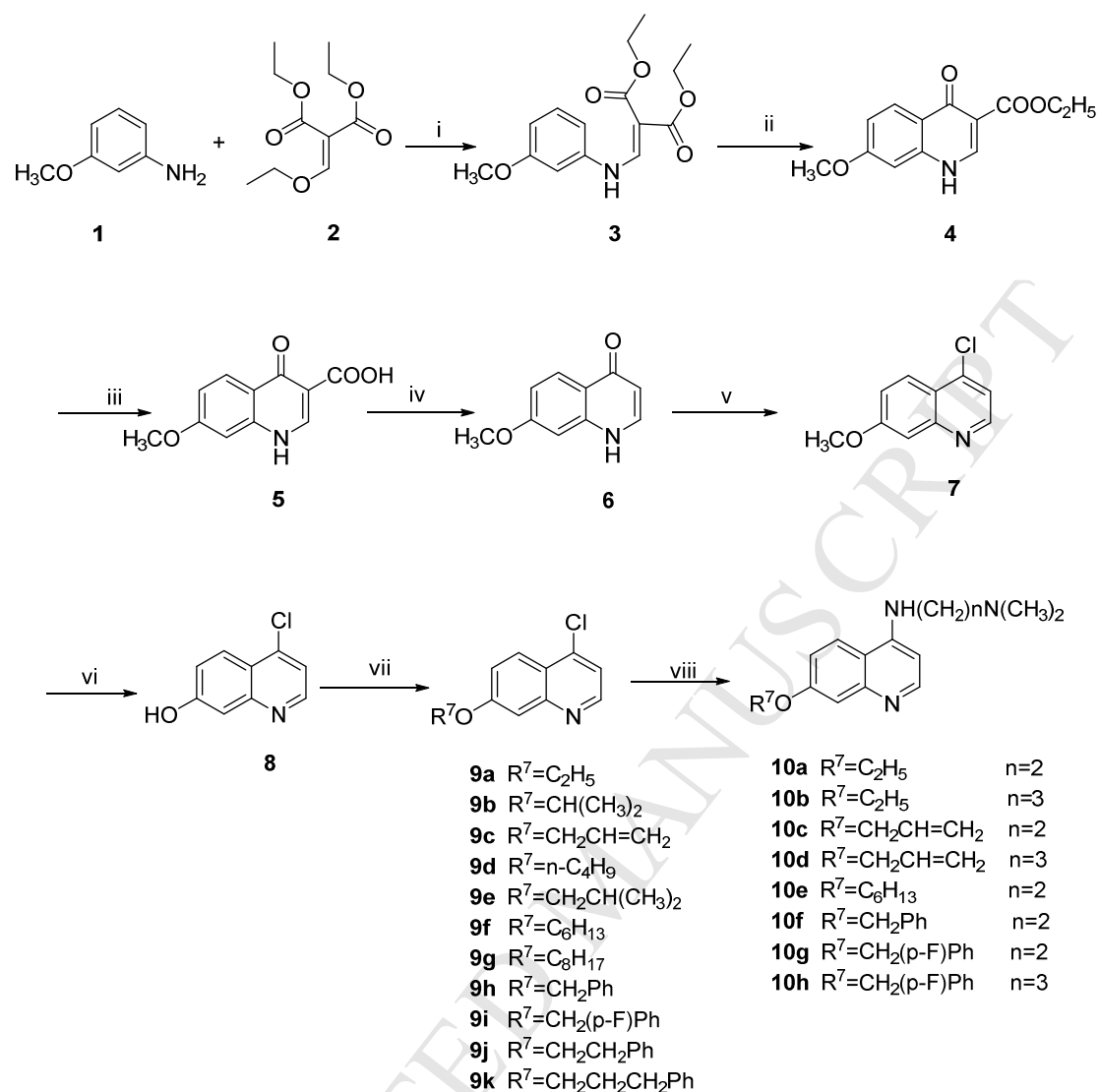
Table 1 Cytotoxic activities of compounds **7**, **9a-k** and **10a-h** *in vitro*^c

Compounds	IC ₅₀ (μM) ^a						
	HCT-116 ^b	RKO	DLD1	HepG2	BGC-823	NCI-H1650	SK-OV-3
7	8.82	9.65	>10	6.07	>10	8.16	>10
9a	3.16	3.87	2.75	2.66	3.91	3.34	3.46
9b	2.59	2.69	3.24	2.05	2.63	2.31	3.06
9c	2.57	2.46	2.89	2.77	2.93	2.28	4.03
9d	2.74	3.05	3.78	2.64	3.61	2.57	4.13
9e	2.49	2.68	3.10	2.25	3.03	2.10	3.19
9f	2.44	2.72	2.66	2.42	2.38	2.08	>10
9g	2.82	3.64	4.50	2.64	4.30	3.24	4.30
9h	2.47	2.41	3.27	2.68	5.17	2.72	5.17
9i	2.07	1.98	3.23	3.01	2.78	2.23	2.78
9j	2.18	2.56	3.38	3.31	2.01	2.30	2.01
9k	0.80	1.42	2.14	1.78	2.37	0.63	3.61
10a	2.57	3.65	6.24	5.68	2.52	3.49	4.62
10b	3.38	5.24	8.54	5.86	9.81	3.83	6.78
10c	0.86	1.27	1.53	1.66	1.36	0.93	1.56
10d	2.10	3.56	5.18	3.99	6.68	3.12	4.25
10e	0.85	1.12	1.87	1.37	1.09	0.93	1.86
10f	1.98	2.35	2.14	3.12	1.25	1.62	2.35
10g	0.37	0.58	0.81	0.79	0.89	0.78	0.89
10h	0.74	1.23	2.54	1.57	0.49	0.94	1.28
11	>10	>10	>10	>10	>10	>10	>10
Cisplatin	12.8	10.2	8.71	10.7	9.7	11.6	8.5

^aCytotoxicity as IC₅₀ for each cell line, is the concentration of compound which reduced by 50% the optical density of treated cells with respect to untreated cells using the MTT assay.

^bCell lines include human laryngeal carcinoma (HCT-116, RKO and DLD1), liver carcinoma (HepG2), gastric carcinoma (BGC-823), non-small-cell lung carcinoma (NCI-H1650) and ovarian carcinoma (SK-OV-3).

^cData represent the mean values of three independent determinations.



Scheme 1 Synthesis of compounds **7**, **9a-k** and **10a-h**. (i) stirred at 100°C; (ii) diphenyl ether, reflux; (iii) NaOH/ethanol, reflux; (iv) diphenyl ether, reflux; (v) POCl₃, reflux; (vi) 48% HBr, reflux; (vii) DMF, NaH, alkyl halogenide, stirred at RT; (viii) NH₂(CH₂)_nN(CH₃)₂, reflux.

Research highlights

- ✓ A series of new quinolines derivatives was synthesized and evaluated as antitumor agent.
- ✓ Compound **10g** was found to be the most potent antiproliferative agent.
- ✓ Compound **10g** triggered p53/Bax-dependent colorectal cancer cell apoptosis by activating p53 transcriptional activity.
- ✓ Compound **10g** effectively inhibited tumor growth in a colorectal cancer xenograft model in nude mice.